ARTICLE OPEN

Check for updates

Circulating lipids are related to longitudinal changes of ATN biomarkers for Alzheimer's disease

Jun Pyo Kim[1,2,57], Kwangsik Nho[1,57], Tingting Wang[3,4], Kevin Huynh[3,4,5], Matthias Arnold[6,7], Shannon L. Risacher[1], Paula J. Bice[1], Xianlin Han[8], Bruce S. Kristal[9], Colette Blach[10], Rebecca Baillie[11], Gabi Kastenmüller[7,12], Peter J. Meikle[3,4,5], Andrew J. Saykin[1]✉, Rima Kaddurah-Daouk[6,13,14]✉, for the Alzheimer's Disease Neuroimaging Initiative* and Alzheimer's Disease Metabolomics Consortium (ADMC)*

Investigating the relationship of circulating lipidome profiles with cross-sectional and longitudinal changes of central Alzheimer's disease (AD) biomarkers, including amyloid/tau/neurodegeneration (A/T/N), can provide a holistic view between the lipidome and AD pathophysiology. In this study, we quantified a total of 749 plasma lipid species at baseline using liquid chromatography–mass spectrometry and performed cross-sectional and longitudinal association analysis of plasma lipidome profiles with longitudinal A/T/N biomarkers for AD in the Alzheimer's Disease Neuroimaging Initiative cohort (N = 1395). We identified several lipid species, classes, and network modules of correlated lipids that were significantly associated with cross-sectional and longitudinal changes of A/T/N biomarkers. Notably, we identified lysoalkylphosphatidylcholine (LPC(O)) as associated with cross-sectional "A/N" biomarkers at the lipid species, class, and module levels. Also, Phosphatidylethanolamine (PE) ethers were associated with A/T/N biomarkers in the species level and with "N" biomarkers in the class and module levels. G_{M3} ganglioside showed association with cross-sectional and longitudinal changes of "N" biomarkers at the species and class levels. Furthermore, 20 lipid species, out of all 57 species identified as associated with "less severe" AD biomarkers, contained docosahexaenoic acid (DHA), indicating that the previously reported beneficial effects of DHA on AD were significant at the central biomarker level. In conclusion, our approach linking peripheral metabolic changes with brain metabolic, structural, and functional states strengthens evidence from previous studies that were performed using only clinical AD diagnosis. Importantly, our study also enabled identification of novel lipids that play potential roles in progression of AD pathophysiology, suggesting dysregulation of lipid metabolic pathways as precursors to AD development and progression.

Molecular Psychiatry; https://doi.org/10.1038/s41380-026-03626-z

INTRODUCTION

Alzheimer's disease (AD) is a neurodegenerative disorder characterized by a cascade of pathological processes, from the accumulation of misfolded proteins such as β-amyloid (Aβ) and hyperphosphorylated tau (p-Tau) to the eventual development of neurodegeneration [1]. Despite decades of research efforts, a significant portion of AD pathogenesis remains uncertain. To understand the complex nature of AD, multiple levels of omics characteristics of the disease have been investigated [2], lipidomics being one of them. Lipidomics is the systems-level analysis of lipids and factors that interact with lipids [3]. The involvement of lipids in AD pathogenesis has been suggested in many previous studies. In particular, alterations of phospholipid, plasmalogens, ceramide, ganglioside, and sulfatide levels in the brain have been observed [4–10]. Also, several recent studies have demonstrated alterations of blood lipidome profiles in AD [11–15]. Furthermore, in a recent lipidomics study using two large cohorts, the Australian Imaging, Biomarkers and Lifestyle (AIBL) study and the Alzheimer's Disease Neuroimaging Initiative (ADNI), a total of 218 lipid species were identified as associated with prevalent or incident AD [16].

[1]Center for Neuroimaging, Radiology and Imaging Sciences, and the Indiana Alzheimer's Disease Research Center, Indiana University School of Medicine, 340 West 10th St, Indianapolis IN 46202, USA. [2]Department of Neurology, Samsung Medical Center, 81 Irwon-ro, Seoul 06351, Korea. [3]Baker Heart and Diabetes Institute, 75 Commercial Rd, Melbourne, VIC 3004, Australia. [4]Baker Department of Cardiometabolic Health, University of Melbourne, Grattan Street, Parkville, VIC 3010, Australia. [5]Department of Cardiovascular Research Translation and Implementation, La Trobe University, Plenty Road and, Kingsbury Dr, Bundoora, VIC 3086, Australia. [6]Department of Psychiatry and Behavioral Sciences, Duke University, Durham, NC 27708, USA. [7]Institute of Computational Biology, Helmholtz Zentrum München, German Research Center for Environmental Health, Ingolstädter Landstr. 1, 85764 Neuherberg, Germany. [8]University of Texas Health Science Center at San Antonio, 7703 Floyd Curl Dr, San Antonio, TX 78229, USA. [9]Division of Sleep and Circadian Disorders, Department of Medicine, Brigham and Women's Hospital, and Division of Sleep Medicine, Harvard Medical School, 25 Shattuck St, Boston, MA 02115, US. [10]Duke Molecular Physiology Institute, Duke University, Durham, NC 27708, USA. [11]Rosa & Co LLC, 751 Laurel St. Ste. 127, San Carlos, California 94070, USA. [12]German Center for Diabetes Research (DZD), Ingolstädter Landstraße 1, 85764 Neuherberg, Germany. [13]Duke Institute of Brain Sciences, Duke University, Durham, NC 27708, USA. [14]Department of Medicine, Duke University, Durham, NC 27708, USA. [57]These authors contributed equally: Jun Pyo Kim, Kwangsik Nho. *A list of authors and their affiliations appears at the end of the paper. Data used in preparation of this article were obtained from the Alzheimer's Disease Neuroimaging Initiative (ADNI) database (adni.loni.usc.edu). As such, the investigators within the ADNI contributed to the design and implementation of ADNI and/or provided data but did not participate in analysis or writing of this report. Data used in preparation of this article were generated by the Alzheimer's Disease Metabolomics Consortium (ADMC), a part of the Accelerating Medicines Partnership for Alzheimer's Disease (AMP-AD). ✉email: asaykin@iu.edu; rima.kaddurahdaouk@duke.edu

Received: 12 March 2024 Revised: 23 February 2026 Accepted: 17 April 2026
Published online: 16 June 2026

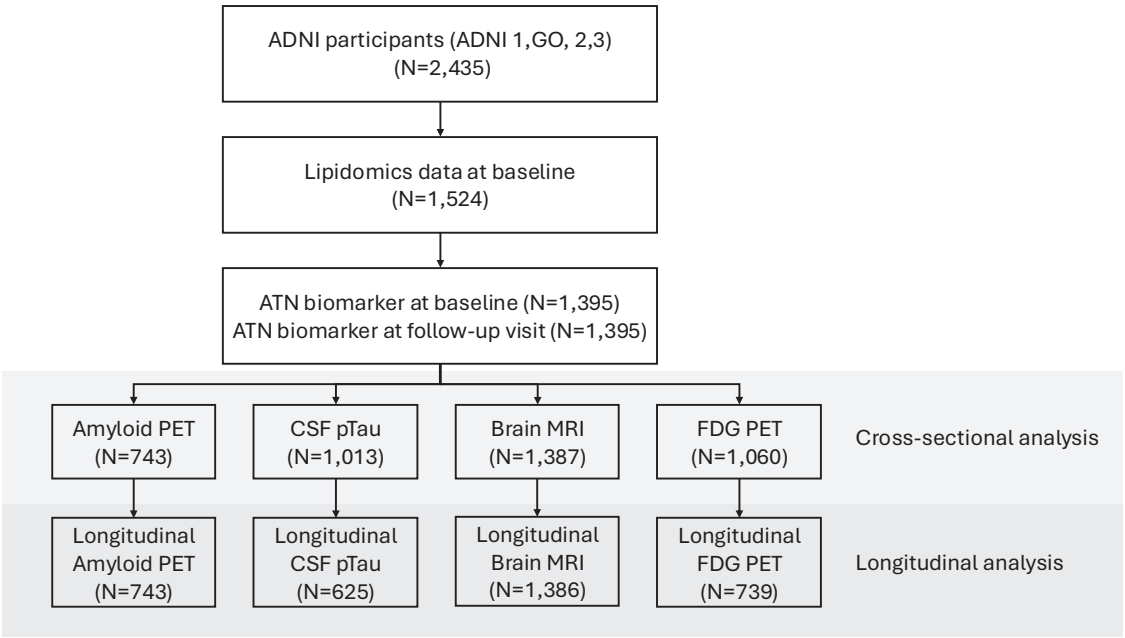

Fig. 1 Study design and analytic workflow of the ADNI lipidomics cohort. ADNI Alzheimer's Disease Neuroimaging Initiative, PET Positron emission tomography, CSF cerebrospinal fluid, MRI Magnetic resonance imaging, FDG = ^{18}F-Fluorodeoxyglucose.

Advances in AD biomarker research have led to the shift of AD diagnosis from clinical syndrome to biological process. AD-related biomarkers can be grouped into those of β-amyloid, hyperphosphorylated tau, and neurodegeneration (A/T/N) [17]. In this regard, the concept of an A/T/N classification system was included in the 2018 National Institute of Aging and Alzheimer's Association Research Framework [18] and has been widely used in AD research since then. Central biomarkers in this study refer to the established A/T/N biomarkers measured by PET, CSF, and MRI, as defined by recent international consensus criteria [19, 20]. Abnormalities in these biomarkers are central to the biological classification of AD and are strongly predictive of subsequent cognitive decline and progression to dementia, as demonstrated in large-scale longitudinal studies [18, 21]. Recent clinical guidelines and major therapeutic trials now rely on these biomarkers for both disease definition and regulatory approval of new treatments. A few existing studies examining the associations between A/T/N biomarkers for AD and blood lipidome have employed techniques that have limited resolution of lipid species [22–24] and have focused primarily on cross-sectional associations.

Here, we investigated associations of circulating lipidome with cross-sectional and longitudinal central A/T/N biomarkers for AD using a recently developed lipidomics platform covering 749 lipid species across 46 classes that focuses on lipid and lipid-like compounds utilizing chromatographic separation and quantitation. We examined the main effect and interactions of sex and *APOE* ε4 carrier status on circulating lipids at the lipid species and lipid class levels. Finally, we identified network modules of correlated lipids and performed association analyses between the modules and cross-sectional and longitudinal A/T/N biomarkers for AD.

SUBJECTS AND METHODS

Participants

Data used in the preparation of this article were obtained from the Alzheimer's Disease Neuroimaging Initiative (ADNI) database (adni.loni.usc.edu). Participants were included in the analysis if they had baseline lipidomics data and ATN biomarker results available at baseline, with or without additional ATN biomarker results at follow-up visits (Fig. 1). The ADNI was launched in 2003 as a public-private partnership, led by Principal Investigator Michael W. Weiner, MD. The primary goal of ADNI has been to test whether serial magnetic resonance imaging (MRI), positron emission tomography (PET), other biological markers, and clinical and neuropsychological assessment can be combined to measure the progression of mild cognitive impairment (MCI) and early Alzheimer's disease (AD). Inclusion and exclusion criteria, clinical and neuroimaging protocols, and other information about ADNI can be found at www.adni-info.org. Demographic information, apolipoprotein E (APOE) and clinical information are available and were downloaded from the ADNI data repository (www.loni.usc.edu/ADNI/). Written informed consent was obtained according to the Declaration of Helsinki at the time of enrollment, and consent forms were approved by the Institutional Review Board at each of the ADNI participating sites. The ADNI study is coordinated by the University of Southern California.

Amyloid/Tau/Neurodegeneration biomarkers for AD

Baseline and longitudinal amyloid PET scan, CSF biomarker, FDG PET scan, and MRI scan data were downloaded from the LONI database (https://adni.loni.usc.edu/). For CSF biomarker data, we used the UPENNBIOMK9 dataset, which was generated using the validated and highly automated Roche Elecsys electrochemiluminescence immunoassays [21]. CSF p-tau values were additionally log-transformed. For FDG-PET, MRI, and amyloid PET phenotypes, raw imaging data were downloaded and processed by established neuroimaging processing protocols. For FDG-PET phenotypes, we used an ROI-based measure of average uptake across the left and right temporal regions derived from preprocessed scans (co-registered, averaged, standardized image and voxel size, uniform resolution) and intensity-normalized using the pons/vermis region to obtain standardized uptake value ratio means [25]. T1-weighted brain MRI scans were downloaded from the ADNI database. As detailed in previous studies [26], FreeSurfer software was used to process T1-weighted brain MRI scans and extract region of interest (ROI)-based imaging phenotypes. We used a global cortical amyloid deposition measured from amyloid PET scans as biomarkers of β-amyloid ("A"). We used CSF phosphorylated tau (p-tau) levels as the biomarker of fibrillary tau ("T"). Both hippocampal volume and temporal lobar FDG uptake were used as a biomarker of neurodegeneration ("N").

Measurement of circulating lipid profiles

We acquired lipidomic profiles (749 lipid species from 46 lipid classes, Supplementary Table 1.) of all plasma samples using our recently expanded, targeted lipidomic profiling strategy based on reverse phase

Table 1. Clinical characteristics.

	All	Amyloid PET	CSF	FDG PET	MRI
N	1395	743	1013	1060	1387
Visit ≥ 2 (N(%))	-	691(93.0)	633(62.5)	739(69.7)	1386(99.9)
Age, years (Mean(SD))	73.62 (7.10)	72.35 (7.22)	73.11 (7.26)	73.16 (7.16)	73.60 (7.11)
Sex, male (N(%))	768 (55.1)	392 (52.8)	556 (54.9)	593 (55.9)	764 (55.1)
Education, years (Mean(SD))	15.99 (2.81)	16.30 (2.63)	16.09 (2.75)	16.11 (2.76)	15.99 (2.82)
APOE ε4 carrier (N(%))	656 (47.0)	337 (45.4)	464 (45.8)	498 (47.0)	655 (47.2)

PET positron emission tomography, *CSF* cerebrospinal fluid, *FDG* fluorodeoxyglucose, *MRI* magnetic resonance imaging, *SD* standard deviation, *APOE* apolipoprotein E.

liquid chromatography coupled to an Agilent 6495 C QqQ mass spectrometer. In terms of the lipid extraction and LC-MS/MS methodology, we used scheduled multiple reaction monitoring (MRM), as previously described [27], with the addition of approximately 200 novel lipid species from 17 lipid classes [28]. Further details about our latest lipid profiling methodology are described on our laboratory website (https://metabolomics.baker.edu.au/method/).

Calculation of omega-3 and ceramide-based indices

While the conventional omega-3 index is typically measured as the percentage of EPA and DHA in erythrocyte membranes, we derived surrogate indices from plasma lipidomics profiles, providing an indirect estimate using the sum of relevant phospholipid species. Specifically, for each participant, we calculated the "omega-3 index surrogate" as the sum of relative abundances (expressed as a percentage of total measured phospholipid species) of all phospholipid species containing eicosapentaenoic acid (EPA, 20:5n-3), docosapentaenoic acid (DPA, 22:5n-3), or docosahexaenoic acid (DHA, 22:6n-3) at either sn-1 or sn-2 position [29].

The Ceramide-based Cardiovascular Risk Score 2 (CERT2) was calculated for each participant using the method described by Hilvo et al [30]. Four lipid variables were used: Cer(d18:1/24:1)/Cer(d18:1/24:0), Cer(d18:1/16:0)/PC(16:0/22:5), Cer(d18:1/18:0)/PC(14:0/22:6), and PC(16:0/16:0). For each variable, participants were assigned 0–3 points according to the quartile in which their value fell within the study population (Q1 = 0, Q2 = 1, Q3 = 2, Q4 = 3). The CERT2 score was calculated as the sum of these points (range 0–12), with higher scores indicating increased ceramide-based cardiovascular risk.

Statistical analysis

We used linear regression models to examine the associations of individual lipids, lipid classes, and lipid modules with A/T/N biomarkers at baseline. For longitudinal analysis of A/T/N biomarkers, we used linear mixed effects models with a random intercept and slope. For class-level analysis, we used the first principal component of each pre-defined class (Supplementary Table 1) to represent the class. To examine the contribution of fatty acid composition within plasmalogen species, we constructed composite scores for omega-3 and omega-6 plasmalogens by calculating the first principal component for each group containing the respective fatty acids. The principal component was obtained using the psych R package. To detect network-based correlation modules in lipidome data, we used the WGCNA R package that utilizes the hierarchical clustering and dynamic tree cut algorithm. The biweight midcorrelation method was used to calculate the correlation between lipids with a soft-thresholding power of 7. The minimum number of lipids within modules was set to 5. The levels of lipids in a module were represented by the module eigen-lipid (ME), which is defined as the first principal component of the lipid matrix of the corresponding module. We examined the interactions of sex and *APOE* ε4 carrier status on circulating lipids, lipid classes and lipid molecules showing significant associations.

All linear models and linear mixed effects models were adjusted for age, sex, the number of *APOE* ε4 alleles, body mass index (BMI), fasting status, levels of clinical lipids (triglyceride, HDL cholesterol, total cholesterol), statin use, and omega-3 use. For association analysis with hippocampal volume, educational attainment, intracranial volume, and magnetic field strength were additionally included as covariates. Taking multiple testing into account, all *p*-values were adjusted using a false discovery rate (FDR) correction with the Benjamini-Hochberg procedure.

For cross-sectional analyses, we used the following linear regression models:

- ATN_biomarker ~ lipid_level + covariates
- ATN_biomarker ~ lipid_class_PC1 + covariates
- ATN_biomarker ~ lipid_module_ME + covariates
- (For interaction analysis) ATN_biomarker ~ lipid_level * sex (or APOE4_status) + covariates

For longitudinal analyses, we used the following linear mixed-effects regression models:

- ATN_biomarker ~ lipid_level * Years.bl + covariates + (Years.bl|RID)
- ATN_biomarker ~ lipid_class_PC1 * Years.bl + covariates + (Years.bl|RID)
- ATN_biomarker ~ lipid_module_ME * Years.bl + covariates + (Years.bl|RID)
- (For interaction analysis) ATN_biomarker ~ lipid_level * Years.bl * sex (or APOE4_status) + covariates + (Years.bl|RID)

where Years.bl refers to years from baseline and RID is the individual subject ID. All covariates (age, sex, education, APOE ε4 status, BMI, statin use, omega-3 supplementation, triglyceride, HDL, total cholesterol, and fasting status, intracranial volume, and magnetic field strength) were included as fixed effects.

For whole brain imaging analysis, the processed amyloid PET and FDG PET images were used to perform a voxel-wise statistical analysis of the effect of lipid network modules on brain amyloid-β deposition and brain glucose metabolism, respectively, across the whole brain using SPM12 (www.fil.ion.ucl.ac.uk/spm/). For surface-based whole brain analysis, the SurfStat software package (www.math.mcgill.ca/keith/surfstat/) was used to perform a multivariable analysis of cortical thickness to examine the effect of lipid network modules on brain structural atrophy on a vertex-by-vertex basis using a general linear model (GLM) approach [31]. We performed a multivariable regression analysis using the same covariates included in the linear models for cross-sectional analysis. For cortical thickness, MRI magnetic field strength and intracranial volume (ICV) were added as additional covariates. In the voxel-wise whole brain analysis, the significant statistical parameters were selected to correspond to a threshold of $p < 0.05$ (FDR-corrected). In the surface-based whole brain analysis, an adjustment for multiple comparisons was performed using the random field theory correction method with $p < 0.05$ adjusted as the level for significance [32, 33].

RESULTS

Study sample

A total of 1395 individuals were included in the analysis. The characteristics of individuals used in the cross-sectional and longitudinal analysis are shown in Table 1.

Cross-sectional association analysis between lipids and A/T/N biomarkers at baseline

Individual lipid species associated with A/T/N biomarkers at baseline. The results of cross-sectional analysis at baseline between lipid levels and A/T/N biomarkers for AD after FDR correction are shown in Fig. 2 (Supplementary Table 2). A total of nine lipids across four classes (sphingomyelin [SM], lysophosphatidylcholine [LPC], alkylphosphatidylethanolamine [PE(O)],

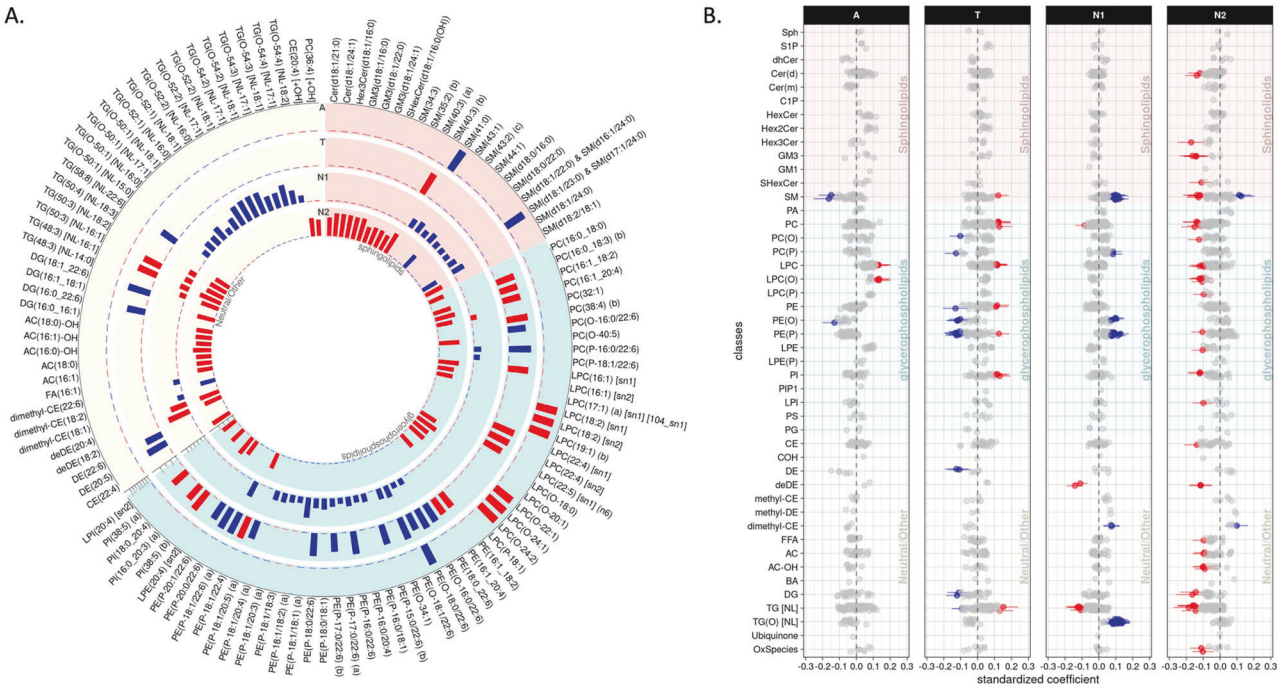

Fig. 2 Lipid species levels: association results of lipid species with A/T/N biomarkers at baseline. A The bar plots from the outermost to innermost circles showed association results between lipid species and A(Amyloid PET)/T(CSF pTau)/N1(MRI)/N2(FDG PET) biomarkers at baseline, respectively. The height of the bars represents the log-transformed FDR corrected *p* values. **B** The forest plots showed lipid species-wise cross-sectional association results arranged by lipid classes. Red colors represent that higher levels of the red colored lipid species were significantly associated with worse AD biomarkers, and blue colors represent that lower levels of the blue colored lipid species were significantly associated with worse AD biomarkers.

and lysoalkylphosphatidylcholine [LPC(O)]) were identified as significantly associated with the "A" biomarker. Also, 36 lipids across 12 classes (SM, PC, alkylphosphatidylcholine [PC(O)], alkenylphosphatidylcholine [PC(P)], LPC, phosphatidylethanolamine [PE], PE(O), alkenylphosphatidylethanolamines [PE(P)], phosphatidylinositol [PI], dehydrocholesteryl ester [DE], diacylglycerol [DG], and triacylglycerol [TG]) showed significant associations with the "T" biomarker. For the "N" biomarker, 94 lipids across 26 classes were significantly associated with hippocampal volume or brain glucose metabolism. The classes included Cer(d), trihexosylceramide [Hex3Cer], G_{M3} gangliosides [GM3], sulfatide [SHexCer], SM, PC, PC(O), PC(P), LPC, LPC(O), lysoalkenylphosphatidylcholine [LPC(P)], PE(O), PE(P), LPE, PI, lysophosphatidylinositol [LPI], CE, dehydrodesmosteryl ester [deDE], dimethylcholesteryl ester [dimethyl-CE], free fatty acid [FFA], acylcarnitine [AC], hydroxylated acylcarnitine [AC-OH], DG, TG, alkyldiacylglycerol [TG(O)], and oxidized lipids.

We identified a significant interaction of *APOE* ε4-carrier status with LPC(O-24:1) levels in association with the "A" biomarker after FDR correction ($\beta_{interaction}$(95% confidence interval[CI]) 0.134(0.065 – 0.202), $p_{FDR} = 0.034$). LPC(O-24:1) showed a significant association with the "A" biomarker in the *APOE* ε4-carrier group ($\beta_{interaction}$(95%CI) 0.242(0.133 – 0.352), $p_{FDR} = 0.007$), but the association was not significant in the *APOE* ε4 non-carriers ($\beta_{interaction}$(95%CI) 0.059(−0.045 – 0.164), $p_{FDR} = 0.924$). However, we did not identify any significant interactions of sex with lipids in the association with A/T/N biomarkers.

Lipid classes associated with A/T/N biomarkers at baseline. In the class-level association analysis, six classes (Hex2Cer, LPC, LPC(O), LPC(P), LPE, and DE) were identified as significantly associated with the "A" biomarker (Fig. 3, Supplementary Table 3). For the "T" biomarker, none of the classes showed any significant associations at the class level. For the "N" biomarker, five classes (PE(P), deDE, methyl-DE, dimethyl-CE, and TG(O)) were significantly associated with hippocampal volume, and three classes (GM3, LPC(O), and deDE) were associated with brain glucose metabolism. Although deDE level was significantly associated with N biomarkers, it needs to be noted that levels of deDE species were strongly associated with the use of acetylcholinesterase inhibitors, which are commonly used as treatment in patients with dementia. Lipid classes did not show any significant interactions with sex or *APOE* ε4-carrier status in the association with A/T/N biomarkers for AD.

Lipid network modules associated with A/T/N biomarkers at baseline. Lipid correlation network analysis identified 46 network modules, and the number of lipids in each module ranged from 5 to 62 (excluding the M0 module, which comprises unassigned lipids (Supplementary Table 4). Among these 46 modules, the M39 (lyso-ether lipids), M34 (PUFA-containing lysoglycerophospholipids dominant), M38 (glycosphingolipids (Hex2Cer)), and M3 (LPCs containing odd/branched chain fatty acid) modules were identified as significantly associated with the "A" biomarker, and the M21 (glycerophospholipids with omega-6 fatty acids) module showed a significant association with the "T" biomarker (Fig. 4, Supplementary Table 5). For the "N" biomarker, the M39 (lyso-ether lipids) module was significantly associated with brain glucose metabolism and five modules (M18 (cholesteryl/dehydrocholesteryl esters), M16 (TG(O)s), M15 (ethanolamine ether lipids), M12 (methyl sterol esters), M9 (SM dominant), and M8 (phosphatidylethanolamine plasmalogens containing arachidonic acid)) were significantly associated with hippocampal volume.

The M39 (lyso-ether lipids) module displayed a significant interaction with *APOE* ε4-carrier status in the association with the "A" biomarker after FDR correction ($\beta_{interaction}$(95%CI) 0.203(0.077 – 0.328), $p_{FDR} = 0.006$). The M39 (lyso-ether lipids) module was significantly associated with the "A" biomarker in the *APOE* ε4-

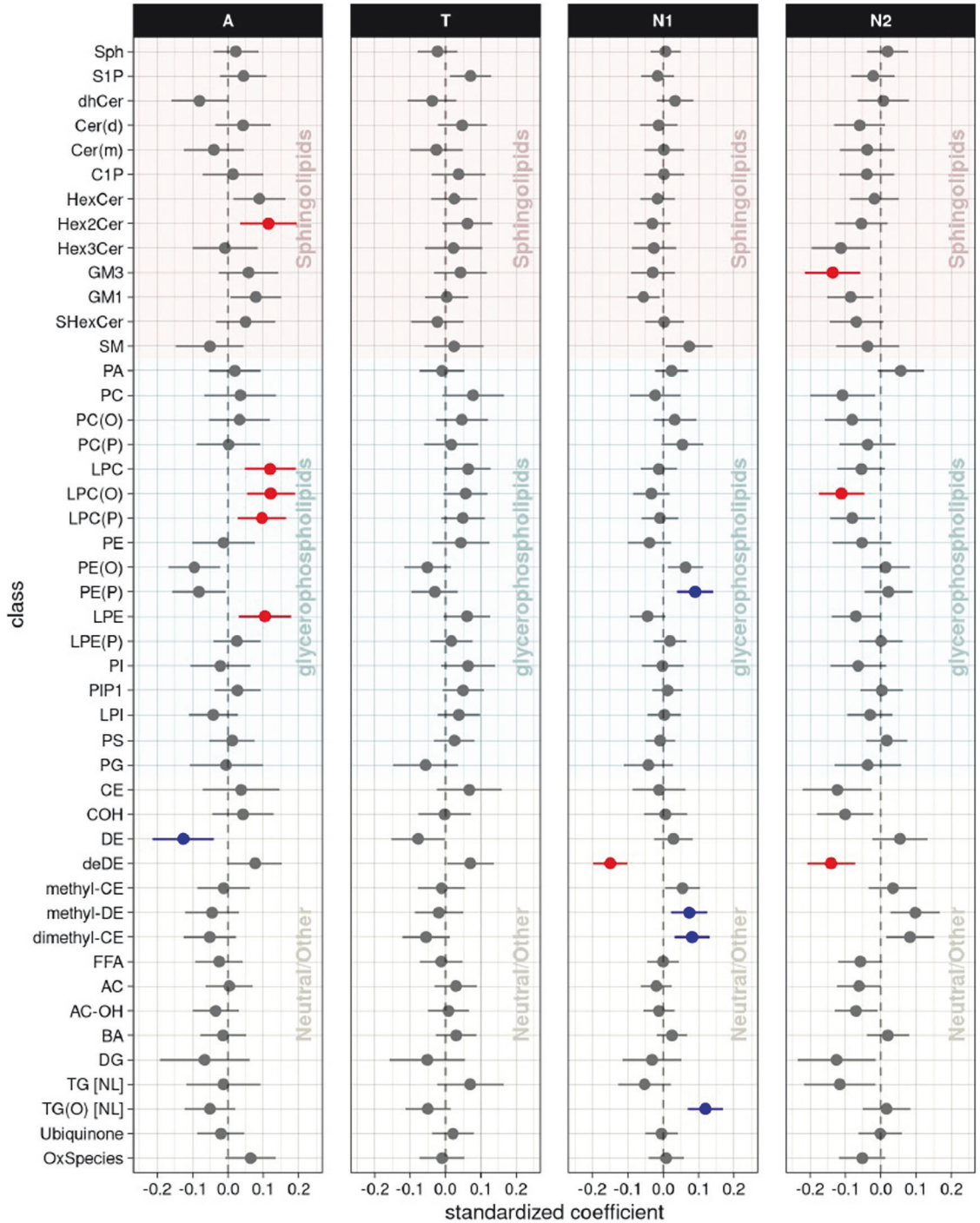

Fig. 3 Lipid class levels: association results of lipid classes with A/T/N biomarkers at baseline. The forest plots showed cross-sectional association results between lipid classes and A(Amyloid PET)/T(CSF pTau)/N1(MRI)/N2(FDG PET) biomarkers at baseline after FDR correction. Red colors represent that higher levels of the red colored lipid classes were significantly associated with worse AD biomarkers, and blue colors represent that lower levels of the blue colored lipid classes were significantly associated with worse AD biomarkers.

carrier group($\beta_{interaction}$(95%CI) 0.242(0.130 – 0.354), $p_{FDR} = 0.001$), but the association was not significant in the *APOE* ε4-non-carrier group ($\beta_{interaction}$(95%CI) 0.038(−0.068 – 0.143), $p_{FDR} = 0.879$). No significant interactions of sex with network modules were identified in the association with A/T/N biomarkers.

In addition, we performed detailed whole-brain association analysis to determine the effect of lipid correlation network modules on brain amyloid-β deposition and brain glucose metabolism on a voxel-wise level and brain structural atrophy on a vertex-wise level (Fig. 5). For amyloid-β deposition, we identified significant associations of four modules (M39 (lyso-ether lipids), M34 (PUFA-containing lysoglycerophospholipids dominant), M38 (Hex2Cer), and M3 (LPCs containing odd/branched chain fatty acid)) with amyloid-β deposition (Fig. 5A). Higher ME values of the four modules were significantly associated with increased amyloid-β deposition in a widespread pattern, especially in the bilateral frontal, parietal, and temporal lobes. For brain glucose metabolism, we identified significant associations for the

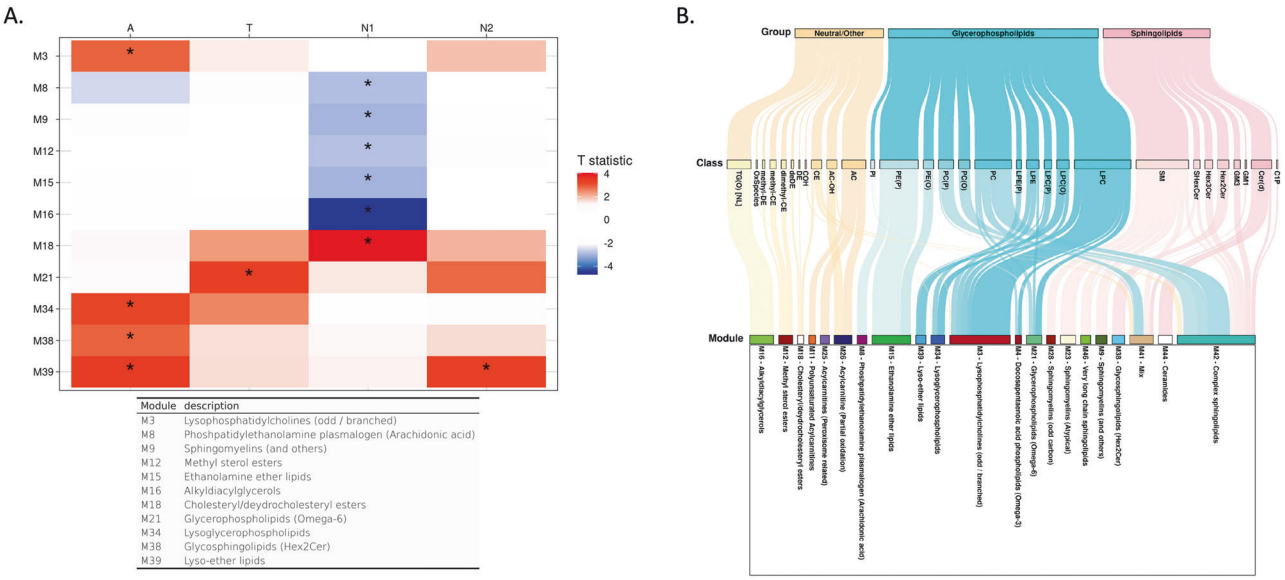

Fig. 4 Lipid network module levels: association results of lipid network modules with A/T/N biomarkers at baseline. A The table showed association results between lipid network modules and A/T/N biomarkers at baseline. Asterisks indicate significant associations after FDR correction. Red colors indicate that higher ME values of the red-colored module were associated with worse AD biomarkers, and blue colors indicate that lower ME values of the blue-colored module were significantly associated with worse AD biomarkers. T statistic values were derived from linear regression analysis and positive T statistic values indicate that higher ME values are associated with worse AD biomarkers. **B** A Sankey diagram was used to visualize clustering of lipid species in the lipid network modules identified as significantly associated with cross-sectional or longitudinal changes of A/T/N biomarkers. FDR False discovery rate, ME module eigen-lipid, AD Alzheimer's disease.

M39 (lyso-ether lipids) module. Higher ME values of the M39 module were significantly associated with reduced brain glucose metabolism in a widespread pattern, especially in the bilateral frontal, parietal, and temporal lobes including the hippocampus (Fig. 5B). For brain structural atrophy, the surface-based whole brain analysis identified significant associations of five modules (M18 (cholesteryl/dehydrocholesteryl esters), M16 (TG(O)s), M15 (ethanolamine ether lipids), M9 (SM dominant), and M8 (phosphatidylethanolamine plasmalogens containing arachidonic acid)) with cortical thickness thinning (Fig. 5C). Lower ME values of the M8, M9, and M15 modules were significantly associated with decreased cortical thickness in the bilateral temporal lobe including the entorhinal cortex. Lower ME values of the M16 module were significantly associated with decreased cortical thickness in a widespread pattern, especially in the bilateral parietal and temporal lobes including the entorhinal cortex. In contrast, higher ME values of the M18 module were significantly associated with decreased cortical thickness in a widespread pattern, especially in the bilateral frontal, parietal and temporal lobes including the entorhinal cortex.

Longitudinal association analysis between lipids at baseline and longitudinal changes of A/T/N biomarkers

Individual lipid species associated with longitudinal changes of A/T/N biomarkers. In the association analysis between baseline lipid levels and longitudinal changes of the "A" and "T" biomarkers, lipids showed no significant associations after FDR correction (Fig. 6, Supplementary Table 6). However, in terms of "N"biomarkers, 15 lipids across eight classes (HexCer, dihexosylceramide [Hex2Cer], GM3, PC, LPC(O), PI, deDE, and AC) showed significant associations with longitudinal changes of hippocampal volume. In addition, a total of 113 lipids across 22 classes (Cer(d), HexCer, Hex2Cer, Hex3Cer, GM1, GM3, SM, PC, PC(O), PC(P), LPC, LPC(O), PE(P), LPE, PI, CE, COH, DE, deDE, AC, AC-OH, and TG) were significantly associated with longitudinal changes of brain glucose metabolism. Of note, among 113 lipids, 26 lipids were also significantly associated with brain glucose metabolism at baseline. The interactions of sex and *APOE* ε4 carrier status with lipids were not significant in the association with longitudinal changes of the A/T/N biomarkers.

Lipid classes associated with longitudinal changes of A/T/N biomarkers. In the class-level longitudinal association analysis, none of the classes were significantly associated with the "A" and "T" biomarkers. However, three classes (GM3, LPC(O), and deDE) were significantly associated with longitudinal changes of hippocampal volume, and 12 classes (Hex3Cer, deDE, PC(O), GM3, GM1, CE, SM, LPC(O), COH, PIP1, PC, and AC) were associated with longitudinal changes of brain glucose metabolism. (Fig. 7, Supplementary Table 7). The interactions of sex and *APOE* ε4-carrier status with lipid classes were not significant in the association with longitudinal changes of the A/T/N biomarkers.

Lipid network modules associated with longitudinal changes of A/T/N biomarkers. There were no significant associations of lipid network modules with longitudinal changes of the "A" and "T" biomarkers, but 13 modules were significantly associated with longitudinal changes of the "N" biomarkers (Fig. 8, Supplementary Table 8). Three modules (M39 (lyso-ether lipids), M18 (cholesteryl/dehydrocholesteryl esters), and M11 (polyunsaturated ACs)) were associated with longitudinal changes of hippocampal volume, and 12 modules (M26 (ACs (partial oxidation)), M25 (ACs (peroxisome-related)), M44 (Cer(d)s), M18 (cholesteryl/deshydrocholesteryl esters), M42 (Complex sphingolipids), M46 (Very long chain sphingolipids), M23 (Atypical SMs), M38 (glycosphingolipids (HEX2CER)), M28 (odd-numbered SMs), M4 (docosapentaenoic acid phospholipids (Omega-3)), M41(mixed), and M39 (lyso-ether lipids)) were identified as significantly associated with longitudinal changes of brain glucose metabolism. For the 13 modules, higher ME values were associated with faster neurodegeneration. Of note, the M39 (lyso-ether lipids) module was significantly associated with the "N" and "A" biomarkers at baseline, and the M18 module was also significantly associated with the "N" biomarker at baseline. The interactions of sex and *APOE* ε4 carrier status with network modules were not significant in association with longitudinal changes of the A/T/N biomarkers.

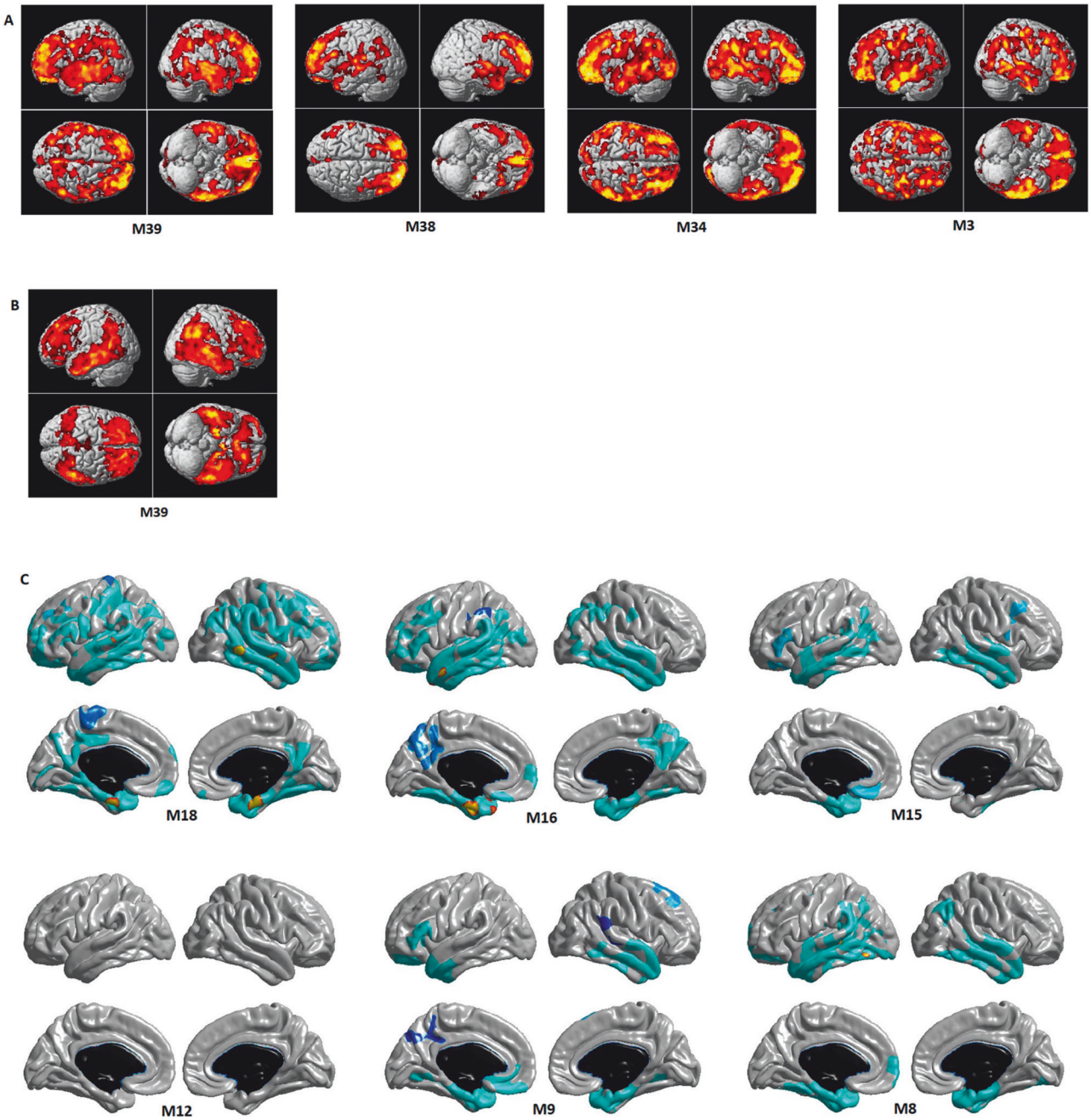

Fig. 5 Voxel- and vertex-wise whole-brain analysis. Detailed whole-brain association analysis for lipid correlation network module levels: association results of network modules with neuroimaging (PET and MRI) biomarkers for AD at baseline for (**A**) brain amyloid deposition using Amyloid PET scans, (**B**) brain glucose metabolism using FDG PET scans, and (**C**) brain structural atrophy using MRI scans. In a voxel-based whole-brain analysis (**A**) and (**B**), colored regions represented significant associations (cluster-wise threshold of FDR-corrected $p < 0.05$). In a surface-based whole-brain analysis (**C**), statistical maps were thresholded using a random field theory for a multiple testing adjustment to a corrected significance level of 0.05. The *p*-value for clusters indicates significant *p* values with the lightest blue color.

Associations of Omega-3 and Omega-6 Plasmalogen Subspecies with AD Biomarkers

Given the potential biological relevance of plasmalogens in AD, we conducted an analysis stratifying plasmalogen species by their constituent fatty acids—specifically, omega-3 and omega-6 polyunsaturated fatty acids (PUFAs). For this purpose, we constructed composite scores for omega-3 and omega-6 plasmalogens using principal component analysis. In cross-sectional analyses, a higher omega-3 plasmalogen composite score was significantly associated with lower amyloid burden ($\beta = -0.081$, 95% CI: -0.158–-0.004, $p = 0.04$) and lower tau pathology ($\beta = -0.113$, 95% CI: -0.181–-0.045, $p = 0.001$), as well as greater hippocampal volume ($\beta = 0.086$, 95% CI: 0.035 to 0.137, $p = 0.001$) (Supplementary Table 9). The omega-6 plasmalogen composite score was associated with increased hippocampal volume ($\beta = 0.058$, 95% CI: 0.009 to 0.108, $p = 0.02$) but showed no significant associations with amyloid, tau, or FDG PET biomarkers. In longitudinal analyses, neither omega-3 nor omega-6 plasmalogen composite scores demonstrated significant associations with longitudinal changes in amyloid, tau, hippocampal volume, or FDG PET measures (all $p > 0.1$).

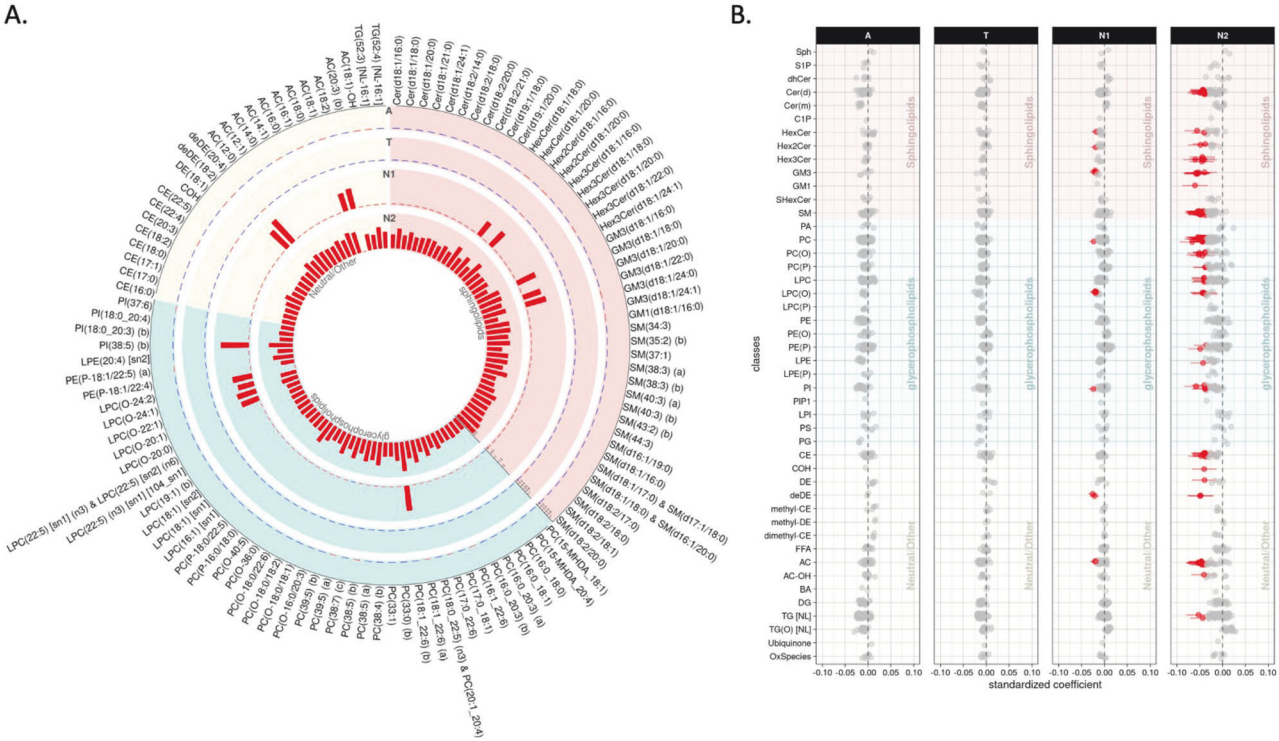

Fig. 6 Lipid species levels: association results of lipids with longitudinal change rates of A/T/N biomarkers for AD. A The bar plots from the outermost to innermost circles showed longitudinal association results between lipid species and longitudinal change rates of A(Amyloid PET)/T(CSF pTau)/N1(MRI)/N2(FDG PET) biomarkers, respectively. The height of the bars represents the log-transformed FDR corrected *p* values. **B** The forest plots showed lipid species-wise longitudinal association results arranged by lipid classes. Red colors represent that higher levels of the red colored lipid species were significantly associated with worse progression of AD biomarkers.

Indices-Based Analysis of Plasma Lipidomics in Relation to AD Biomarkers

To address the broader implications of plasma lipidomics in systemic health, we conducted additional analyses focusing on well-established lipid indices that reflect cardiovascular and metabolic risk profiles. Specifically, we examined the omega-3 index and a ceramide-based risk score (CERT2) that are known to be associated with cardiovascular outcomes. By evaluating the associations of these indices with AD biomarkers, we aimed to bridge systemic lipid metabolism and central neurodegenerative processes. The omega-3 index surrogate (defined as the sum of all measured phospholipid species containing EPA, DPA, and DHA, expressed as a percentage of total measured phospholipids) was significantly and inversely associated with tau pathology in the cross-sectional analysis ($\beta = -0.120$, 95% CI: -0.183–-0.057, $p < 0.001$), while the associations with amyloid, hippocampal volume, and FDG PET were not statistically significant (Supplementary Table 10). In longitudinal analyses, the omega-3 index surrogate did not show significant associations with longitudinal changes in amyloid, tau, hippocampal volume, or FDG PET (all $p > 0.1$).

CERT2 was significantly associated with brain glucose metabolism cross-sectionally ($\beta = -0.093$, $p = 0.005$) and longitudinally ($\beta = -0.031$, $p = 0.029$) but showed no significant association with baseline amyloid or tau levels (Supplementary Table 10). Of note, in longitudinal analysis, CERT2 was associated with longitudinal changes of amyloid and tau accumulation ($\beta = -0.033$, $p = 0.003$ for amyloid; $\beta = -0.017$, $p = 0.018$ for tau).

DISCUSSION

Using an up-to-date lipidomics platform capable of separating a larger number of lipids compared to the platforms used in previous studies, we identified lipid species, lipid classes, and lipid correlation network modules as significantly associated with cross-sectional and longitudinal A/T/N biomarkers for AD. The investigation of the relationship between circulating lipids and central AD biomarkers enabled us to identify lipids having potential roles in the cascade of AD pathogenesis. Studies have shown that pathological changes measured by A/T/N biomarkers preceded the onset of clinical symptoms by years or even decades. Importantly, longitudinal cohort studies have demonstrated that individuals with abnormal A/T/N biomarker profiles experience more rapid cognitive decline and have a substantially higher risk of progressing to clinical dementia compared to those with normal biomarker profiles [20, 21]. Given their central role in disease staging and prognosis, it is important to understand how peripheral factors such as circulating lipidome relate to these biomarkers. Of note, we identified lipid species, lipid classes, and lipid network modules as associated with cross-sectional and longitudinal changes of multiple AD biomarkers, implying their substantial roles in AD pathogenesis and potential roles of lipid profiles as diagnostic and prognostic biomarkers for AD.

We identified the LPC(O) class as associated with baseline amyloid-β deposition (“A”) and neurodegeneration (“N”) at the individual lipid, lipid class, and lipid correlation network module levels. In particular, higher levels of LPC(O) species were associated with higher cortical Aβ deposition and lower glucose metabolism at baseline. Also, the LPC(O) lipids were significantly associated with longitudinal changes of the “N” biomarkers in all three levels. Similar to the cross-sectional association results, higher levels of LPC(O) were associated with more rapid progression of neurodegeneration. These findings are in line with previous studies reporting increases in brain and blood LPC(O) levels in AD patients [34, 35],and a recent study that showed the association between LPC(O) levels and CSF pTau/A42 ratio [36].

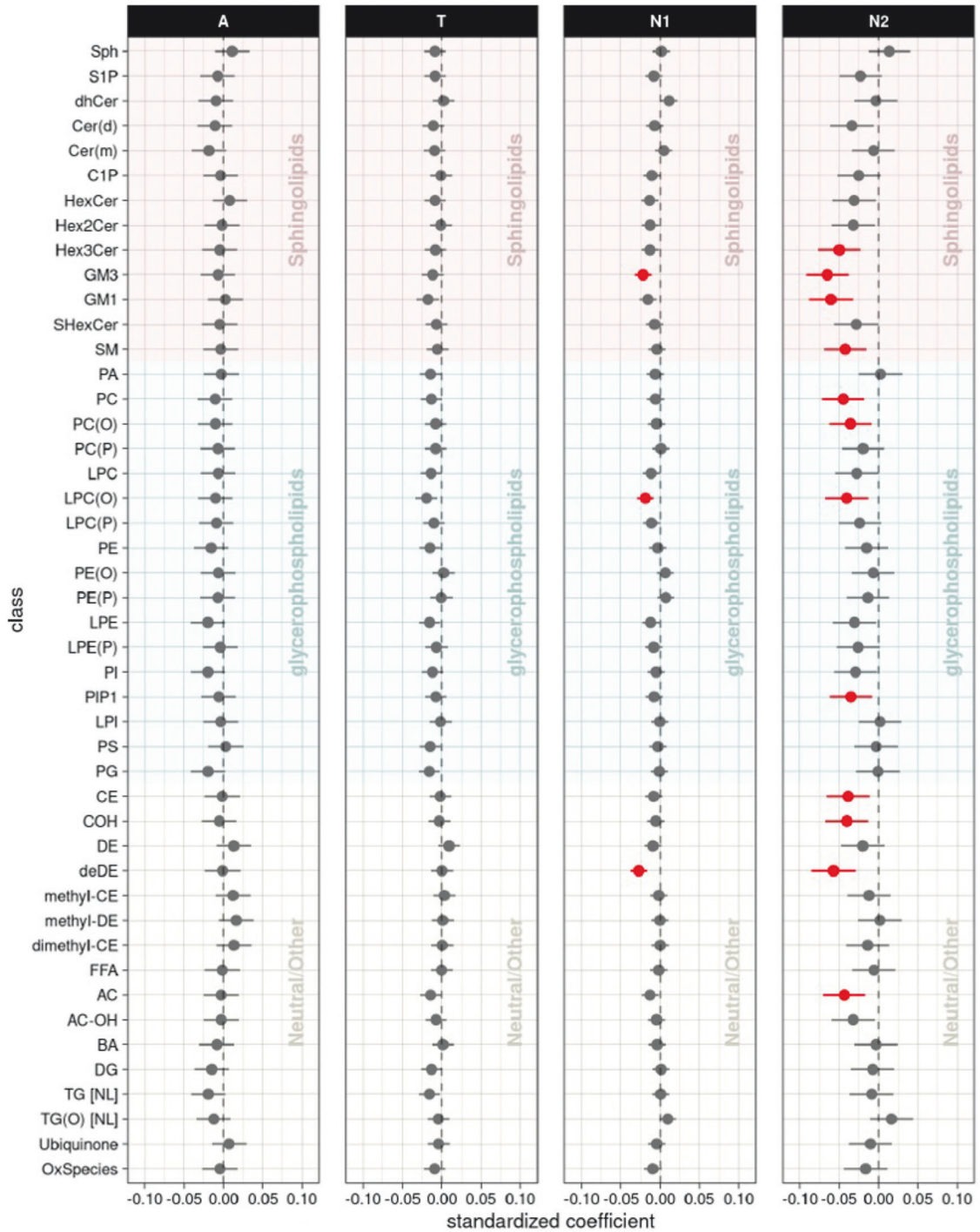

Fig. 7 Lipid class levels: longitudinal association results of lipid classes with longitudinal change rates of A/T/N biomarkers. The forest plots showed longitudinal association results between lipid classes and longitudinal change rates of A(Amyloid PET)/T(CSF pTau)/N1(MRI)/N2(FDG PET) biomarkers after FDR correction. Red colors represent that higher levels of the red colored lipid classes were significantly associated with worse progression of AD biomarkers.

The overall increase of LPC, LPC(O), LPC(P) in subjects with more severe amyloid biomarker in our baseline analysis indicates phospholipase A2 (PLA2) activation, since PLA2 hydrolyzes PC and PC ether species into LPC or LPC ether species. In fact, studies have shown that $A\beta_{1-42}$ activates PLA2 [37–39], which can drive neuroinflammation and oxidative stress in the brain [40, 41].

Another finding was that PE ethers (PE(O), PE(P)) were associated with baseline AD biomarkers in the species level, most of them being associated with more favorable (or less severe) A/T/N biomarker status. Also, in the class and module levels, PE(P) class and two modules related to PE ethers were associated with greater baseline hippocampal volume. However, no significant associations were identified between PE ethers and longitudinal changes of the A/T/N biomarkers in the class or module levels, and only two PE(P) species were associated with faster decline of brain glucose metabolism. PE(P) species (referred to as ethanolamine plasmalogens) are abundant in brain myelin [42] and are known to be decreased in AD, showing negative association with disease

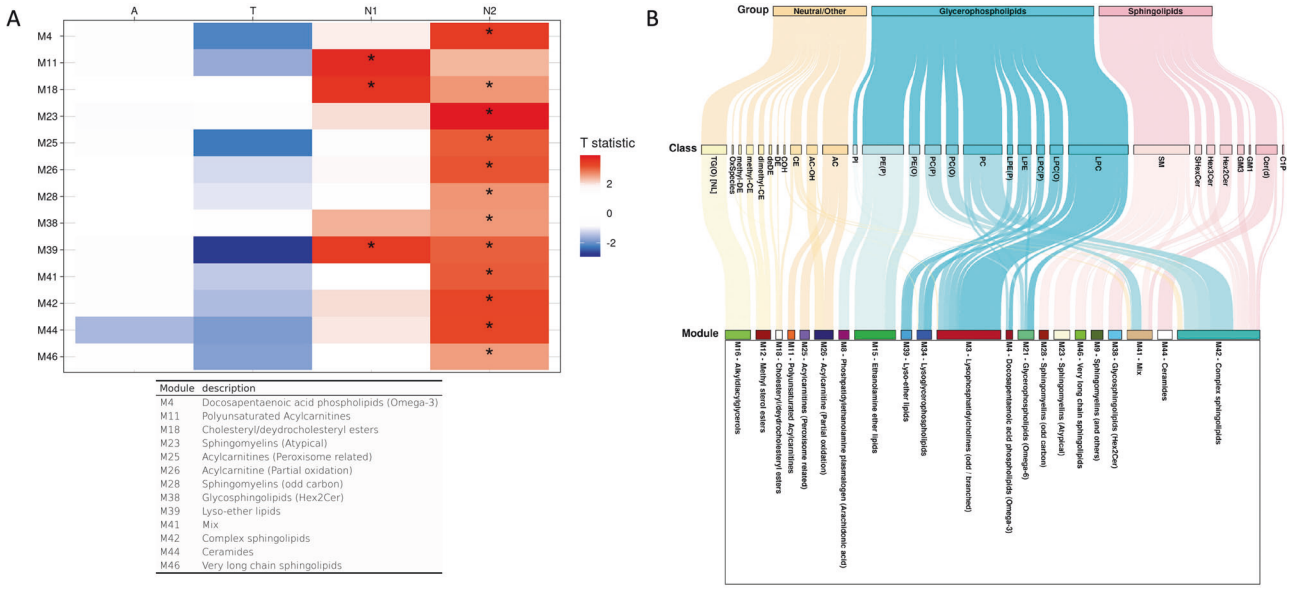

Fig. 8 Lipid network module levels: longitudinal association results of lipid network modules with longitudinal change rates of A/T/N biomarkers. A The table showed longitudinal association results between lipid network modules and longitudinal change rates of A/T/N biomarkers. Asterisks indicate significant associations after FDR correction. Red colors indicate that higher ME values of the red-colored module were associated with worse progression of AD biomarkers, and blue colors indicate that lower ME values of the blue-colored module were significantly associated with worse progression of AD biomarkers. T statistic values were derived from linear mixed effect analysis and positive T statistic values indicate that higher ME values are associated with worse progression of AD biomarkers. **B** A Sankey diagram was used to visualize clustering of lipid species in the lipid network modules identified as significantly associated with cross-sectional or longitudinal changes of A/T/N biomarkers. FDR False discovery rate, ME module eigen-lipid, AD Alzheimer's disease.

severity and CSF Tau [43, 44]. Previous studies have shown that PE(P) species function as endogenous antioxidants through their vinyl ether bonds and protect cells against oxidative stress [45, 46]. The PE(P) species also affect biosynthesis and intracellular transport of cholesterol [47, 48]. The protective effect of PE(P) against AD may have been contributed by these actions, as oxidative stress and intracellular cholesterol trafficking are both known to have roles in AD [49, 50]. PE(O), also known as plasmanylethanolamine, is a precursor of PE(P) [51]. Of note, PE(O-18:0/22:6) showed a significant association with all three A/T/N biomarkers at baseline in our analysis. Unlike PE(P), biological functions of the PE(O) species are not well understood. However, a recent study showed that not only PE(P) but also PE(O) species were negatively associated with prevalent and incident AD [16]. Our results are in line with this study and extend the associations to the AD biomarker level. Our additional analysis revealed that the neuroprotective associations of plasmalogens (PE(P), LPE(P), PC(P), LPC(P)) with AD biomarkers were primarily driven by those species containing omega-3 fatty acids. Specifically, higher omega-3 plasmalogen levels were linked to lower amyloid and tau pathology and to preserved hippocampal volume. These findings highlight the importance of fatty acid composition in modulating the potential protective effects of plasmalogens in AD, suggesting that omega-3-rich plasmalogens may play a key role in AD pathogenesis.

It is notable that 20 lipid species across 7 classes out of all 57 species identified as significantly associated with "less severe" AD biomarker status at baseline contained docosahexaenoic acid (DHA). In particular, the associations of those DHA-containing lipids with the T/N biomarkers were prominent. This type of association cannot be detected at the class level since DHA-containing species exist across the classes. At the module level, one of the modules (M45), in which most members contain DHA, showed marginally significant associations with lower CSF pTau ($p_{FDR} = 0.053$) and larger hippocampal volume ($p_{FDR} = 0.054$). DHA is mainly distributed throughout grey matter and synaptic membranes [52], and is involved in multiple pathways related to neuronal biology, from neuronal development to regulation of synaptic function, neuroprotection and modulation of apoptosis [53, 54]. Studies have shown that individuals with AD have low serum DHA levels, and higher red blood cell DHA is associated with lower risk of incident AD [55, 56]. In line with these studies, there are studies suggesting protective effect of DHA on incident AD or AD-related cognitive decline [57–59]. Our analysis results provide additional evidence of association between DHA and AD on the AD biomarker level. The negative association between DHA and AD biomarkers can be attributed to the anti-inflammatory action of DHA [60]. Also, it has both a direct and indirect antioxidant effect, which can be a potential protective mechanism of DHA against AD-related damage [54, 61].

There were other lipids showing significant associations with the "N" biomarkers. For instance, lipid species in the TG(O) and G_{M3} ganglioside classes were significantly associated with baseline "N" biomarkers at the lipid species and lipid class levels. TG(O) was negatively associated with neurodegeneration, while G_{M3} ganglioside was positively associated with neurodegeneration. TG(O) has been identified as having a protective effect on prevalent and incident AD in a recent multicohort study [16]. Although the direct biological functions of TG(O) are not yet clearly known, TG(O)s are precursors of plasmalogens (PE(P), PC(P)) that play an important role as antioxidants (discussed above) [44, 62]. From a cellular functional perspective, higher levels of peroxisome-derived ether lipids (PC(P), PE(P), PE(O), TG(O)) and related modules (M34, M39) being associated with less neurodegeneration may implicate the role of peroxisomal function in neuroprotection. Peroxisomal alteration in neurodegenerative disease and AD have been suggested in previous studies [63, 64], and peroxisome proliferator-activated receptor (PPAR) has been proposed as a potential treatment target and a link between diabetes and AD [65, 66].

In addition to the significant results in baseline analysis, G_{M3} ganglioside showed significant association with longitudinal changes of the "N" biomarkers at the lipid species and class

levels. In line with the cross-sectional analysis results, higher G_{M3} ganglioside levels were associated with more rapid progression of neurodegeneration. The G_{M3} ganglioside is the first ganglioside in the biosynthetic pathway of the major brain gangliosides. In a mouse model study, the reduction of G_{M3} ganglioside by inhibition of glucosylceramide synthase resulted in stabilized remote memory and lower soluble Aβ in the brain [67]. A previous human study showed that increased levels of the G_{M3} ganglioside species were associated with incident or prevalent AD [8]. Furthermore, in a lipidomics study of the Mayo Clinic cohort, higher G_{M3} ganglioside levels were found to be associated with mild cognitive impairment (MCI), implicating the relevance of G_{M3} gangliosides to early neurodegenerative changes [68]. In addition, another recent lipidomics study identified G_{M3} d18:1/16:0 and G_{M3} d18:1/24:1 as the species showing the strongest positive associations with clinical diagnosis of AD [69]. Notably, these G_{M3} ganglioside species also showed significant associations with cerebral glucose hypometabolism in our study. This convergence of findings across independent cohorts and analytical platforms further underscores the potential role of specific G_{M3} ganglioside species in AD-related neurodegenerative processes.

To further elucidate the broader implications of systemic lipid metabolism in AD pathogenesis, we also examined representative lipidomic indices. The omega-3 index surrogate, defined as the sum of phospholipid species containing EPA, DPA, and DHA as a percentage of total measured phospholipids, was significantly and inversely associated with tau pathology, in line with epidemiological evidence supporting the neuroprotective role of omega-3 fatty acids [70]. The CERT2 score, a validated ceramide-based cardiovascular risk index, showed a significant association with neurodegeneration both cross-sectionally and longitudinally: higher CERT2 scores were related to lower levels of brain glucose metabolism at baseline and faster longitudinal decline of brain glucose metabolism, suggesting that ceramide-driven systemic cardiometabolic risk is linked to progression of brain metabolic dysfunction. Intriguingly, higher CERT2 scores were also associated with slower accumulation of amyloid and tau pathology over time, indicating potentially complex and divergent effects of ceramide metabolism on different aspects of AD pathophysiology. The mechanistic basis for this pattern remains to be elucidated and may reflect differential roles of ceramides in neurodegeneration versus proteinopathy.

Several limitations in the study should be mentioned. First, our findings are observational, and mechanistic studies are needed to identify causal relationships. Another limitation of this study is the lack of large-scale independent data for replication, which precludes a direct assessment of reproducibility. Future work should prioritize the replication of our findings in independent cohorts, which have both lipidomics and longitudinal AD biomarker data. Nevertheless, it is noteworthy that we identified lipids as significantly associated with cross-sectional and longitudinal changes of the A/T/N biomarkers in our comprehensive association analysis.

In conclusion, our study investigating the relationship between circulating lipid profiles and central A/T/N biomarkers for AD has implicated several lipid species, lipid classes, and lipid correlation network modules as potential blood-based AD biomarkers that point to dysregulation of specific lipid metabolic pathways as precursors to AD and linked to the progression of the disease. In particular, we identified lipids showing significant associations across multiple A/T/N biomarkers cross-sectionally and longitudinally, including LPC(O) and PE ether species. We also showed that the previously reported beneficial effects of DHA on AD are significant at the biomarker level. Lastly, our findings using AD endophenotypes strengthen evidence from previous studies that were performed using only an AD diagnosis by linking peripheral metabolic changes with brain metabolic and structural states.

CODE AVAILABILITY

All code essential to the main results is included in the Supplementary Code. There are no restrictions on availability.

REFERENCES

1. Jack JrCR, Knopman DS, Jagust WJ, Shaw LM, Aisen PS, Weiner MW, et al. Hypothetical model of dynamic biomarkers of the alzheimer's pathological cascade. Lancet Neurol. 2010;9:119–28.
2. Badhwar A, McFall GP, Sapkota S, Black SE, Chertkow H, Duchesne S, et al. A multiomics approach to heterogeneity in alzheimer's disease: focused review and roadmap. Brain. 2020;143:1315–31.
3. Wenk MR. The emerging field of lipidomics. Nat Rev Drug Discovery. 2005;4:594–610.
4. Igarashi M, Ma K, Gao F, Kim HW, Rapoport SI, Rao JS. Disturbed choline plasmalogen and phospholipid fatty acid concentrations in alzheimer's disease prefrontal cortex. J Alzheimers Dis. 2011;24:507–17.
5. Han X, Holtzman DM, McKeel DW Jr. Plasmalogen deficiency in early alzheimer's disease subjects and in animal models: molecular characterization using electrospray ionization mass spectrometry. J Neurochem. 2001;77:1168–80.
6. Cheng H, Zhou Y, Holtzman DM, Han X. Apolipoprotein E mediates sulfatide depletion in animal models of alzheimer's disease. Neurobiol Aging. 2010;31:1188–96.
7. Yamamoto N, Igbabvoa U, Shimada Y, Ohno-Iwashita Y, Kobayashi M, Wood WG, et al. Accelerated Abeta aggregation in the presence of GM1-ganglioside-accumulated synaptosomes of aged apoE4-knock-in mouse brain. FEBS Lett. 2004;569:135–9.
8. Han X, Holtzman DM, McKeel DW Jr, Kelley J, Morris JC. Substantial sulfatide deficiency and ceramide elevation in very early alzheimer's disease: potential role in disease pathogenesis. J Neurochem. 2002;82:809–18.
9. Baloni P, Arnold M, Buitrago L, Nho K, Moreno H, Huynh K, et al. Multi-Omic analyses characterize the ceramide/sphingomyelin pathway as a therapeutic target in alzheimer's disease. Commun Biol. 2022;5:1074.
10. Han X, Rozen S, Boyle SH, Hellegers C, Cheng H, Burke JR, et al. Metabolomics in early Alzheimer's disease: identification of altered plasma sphingolipidome using shotgun lipidomics. PLoS One. 2011;6:e21643.
11. Mapstone M, Cheema AK, Fiandaca MS, Zhong X, Mhyre TR, MacArthur LH, et al. Plasma phospholipids identify antecedent memory impairment in older adults. Nat Med. 2014;20:415–8.
12. Chatterjee P, Lim WL, Shui G, Gupta VB, James I, Fagan AM, et al. Plasma phospholipid and sphingolipid alterations in presenilin1 mutation carriers: a pilot study. J Alzheimers Dis. 2016;50:887–94.
13. Whiley L, Sen A, Heaton J, Proitsi P, García-Gómez D, Leung R, et al. Evidence of altered phosphatidylcholine metabolism in alzheimer's disease. Neurobiol Aging. 2014;35:271–8.
14. Wang T, Huynh K, Giles C, Mellett NA, Duong T, Nguyen A, et al. APOE ε2 resilience for alzheimer's disease is mediated by plasma lipid species: analysis of three independent cohort studies. Alzheimers Dement. 2022;18:2151–66.
15. Barupal DK, Baillie R, Fan S, Saykin AJ, Meikle PJ, Arnold M, et al. Sets of coregulated serum lipids are associated with alzheimer's disease pathophysiology. Alzheimers Dement. 2019;11:619–27.
16. Huynh K, Lim WLF, Giles C, Jayawardana KS, Salim A, Mellett NA, et al. Concordant peripheral lipidome signatures in two large clinical studies of alzheimer's disease. Nat Commun. 2020;11:5698.
17. Jack CR Jr., Bennett DA, Blennow K, Carrillo MC, Feldman HH, Frisoni GB, et al. A/T/N: an unbiased descriptive classification scheme for alzheimer disease biomarkers. Neurology. 2016;87:539–47.
18. Jack CR Jr., Bennett DA, Blennow K, Carrillo MC, Dunn B, Haeberlein SB, et al. NIA-AA research framework: toward a biological definition of alzheimer's disease. Alzheimers Dement. 2018;14:535–62.
19. Jack Jr CR, Andrews JS, Beach TG, Buracchio T, Dunn B, et al. Revised criteria for diagnosis and staging of alzheimer's disease: alzheimer's association workgroup. Alzheimer's Dement. 2024;20:5143–69.
20. Therriault J, Schindler SE, Salvadó G, Pascoal TA, Benedet AL, Ashton NJ, et al. Biomarker-based staging of alzheimer disease: rationale and clinical applications. Nat Rev Neurol. 2024;20:232–44.
21. Hansson O, Seibyl J, Stomrud E, Zetterberg H, Trojanowski JQ, Bittner T, et al. CSF biomarkers of Alzheimer's disease concord with amyloid-β PET and predict clinical progression: A study of fully automated immunoassays in BioFINDER and ADNI cohorts. Alzheimers Dement. 2018;14:1470–81.
22. Toledo JB, Arnold M, Kastenmüller G, Chang R, Baillie RA, Han X, et al. Metabolic network failures in alzheimer's disease: a biochemical road map. Alzheimers Dement. 2017;13:965–84.
23. Arnold M, Nho K, Kueider-Paisley A, Massaro T, Huynh K, Brauner B, et al. Sex and APOE ε4 genotype modify the alzheimer's disease serum metabolome. Nat Commun. 2020;11:1148.

24. Varma VR, Oommen AM, Varma S, Casanova R, An Y, Andrews RM, et al. Brain and blood metabolite signatures of pathology and progression in alzheimer disease: a targeted metabolomics study. PLoS Med. 2018;15:e1002482.
25. Landau SM, Harvey D, Madison CM, Koeppe RA, Reiman EM, Foster NL, et al. Associations between cognitive, functional, and FDG-PET measures of decline in AD and MCI. Neurobiol Aging. 2011;32:1207–18.
26. Nho K, Saykin AJ, Alzheimer's Disease Neuroimaging I, Nelson PT. Hippocampal sclerosis of aging, a common alzheimer's disease 'Mimic': risk genotypes are associated with brain atrophy outside the temporal lobe. J Alzheimer's Dis : JAD. 2016;52:373–83.
27. Huynh K, Barlow CK, Jayawardana KS, Weir JM, Mellett NA, Cinel M, et al. High-Throughput plasma lipidomics: detailed mapping of the associations with cardiometabolic risk factors. Cell Chem Biol. 2018;26:71–84.e4.
28. Beyene HB, Olshansky G, T. Smith AA, Giles C, Huynh K, Cinel M, et al. High-coverage plasma lipidomics reveals novel sex-specific lipidomic fingerprints of age and BMI: Evidence from two large population cohort studies. PLOS Biol. 2020;18:e3000870.
29. Wu JH, Lemaitre RN, King IB, Song X, Sacks FM, Rimm EB, et al. Association of plasma phospholipid long-chain ω-3 fatty acids with incident atrial fibrillation in older adults: the cardiovascular health study. Circulation. 2012;125:1084–93.
30. Hilvo M, Meikle PJ, Pedersen ER, Tell GS, Dhar I, Brenner H, et al. Development and validation of a ceramide- and phospholipid-based cardiovascular risk estimation score for coronary artery disease patients. Eur Heart J. 2020;41:371–80.
31. Chung MK, Worsley KJ, Nacewicz BM, Dalton KM, Davidson RJ. General multivariate linear modeling of surface shapes using SurfStat. Neuroimage. 2010;53:491–505.
32. Worsley KJ, Taylor JE, Tomaiuolo F, Lerch J. Unified univariate and multivariate random field theory. NeuroImage. 2004;23:S189–S195.
33. Hayasaka S, Phan KL, Liberzon I, Worsley KJ, Nichols TE. Nonstationary cluster-size inference with random field and permutation methods. Neuroimage. 2004;22:676–87.
34. Ryan SD, Whitehead SN, Swayne LA, Moffat TC, Hou W, Ethier M, et al. Amyloid-β42 signals tau hyperphosphorylation and compromises neuronal viability by disrupting alkylacylglycerophosphocholine metabolism. Proc Natl Acad Sci. 2009;106:20936–41.
35. Dorninger F, Moser AB, Kou J, Wiesinger C, Forss-Petter S, Gleiss A, et al. Alterations in the plasma levels of specific choline phospholipids in alzheimer's disease mimic accelerated aging. J Alzheimer's Dis. 2018;62:841–54.
36. Sakr F, Dyrba M, Bräuer AU, Teipel S, Initiative AsDN. Association of lipidomics signatures in blood with clinical progression in preclinical and prodromal alzheimer's disease. J Alzheimer's Dis. 2022;85:1115–27.
37. Palavicini JP, Wang C, Chen L, Hosang K, Wang J, Tomiyama T, et al. Oligomeric amyloid-beta induces MAPK-mediated activation of brain cytosolic and calcium-independent phospholipase A2 in a spatial-specific manner. Acta neuropathol Commun. 2017;5:1–17.
38. Chalimoniuk M, Stolecka A, Cąkała M, Hauptmann S, Schulz K, Lipka U, et al. Amyloid beta enhances cytosolic phospholipase A2 level and arachidonic acid release via nitric oxide in APP-transfected PC12 cells. Acta Biochimica Polonica. 2007;54:611–23.
39. Anfuso CD, Assero G, Lupo G, Nicotra A, Cannavò G, Strosznajder RP, et al. Amyloid β (1–42) and its β (25–35) fragment induce activation and membrane translocation of cytosolic phospholipase A2 in bovine retina capillary pericytes. Biochimica et Biophysica Acta Mol Cell Biol Lipids. 2004;1686:125–38.
40. Chao C-C, Gutiérrez-Vázquez C, Rothhammer V, Mayo L, Wheeler MA, Tjon EC, et al. Metabolic control of astrocyte pathogenic activity via cPLA2-MAVS. Cell. 2019;179:1483–1498. e1422.
41. Chuang DY, Simonyi A, Kotzbauer PT, Gu Z, Sun GY. Cytosolic phospholipase A2 plays a crucial role in ROS/NO signaling during microglial activation through the lipoxygenase pathway. J Neuroinflammation. 2015;12:1–20.
42. Brites P, Waterham HR, Wanders RJA. Functions and biosynthesis of plasmalogens in health and disease. Biochimica et Biophysica Acta. 2004;1636:219–31.
43. Ginsberg L, Rafique S, Xuereb JH, Rapoport SI, Gershfeld NL. Disease and anatomic specificity of ethanolamine plasmalogen deficiency in alzheimer's disease brain. Brain Res. 1995;698:223–6.
44. Kling MA, Goodenowe DB, Senanayake V, MahmoudianDehkordi S, Arnold M, Massaro TJ, et al. Circulating ethanolamine plasmalogen indices in alzheimer's disease: relation to diagnosis, cognition, and CSF tau. Alzheimers Dement. 2020;16:1234–47.
45. ZOELLER RA, LAKE AC, NAGAN N, GAPOSCHKIN DP, LEGNER MA, LIEBERTHAL W. Plasmalogens as endogenous antioxidants: somatic cell mutants reveal the importance of the vinyl ether. Biochemical J. 1999;338:769–76.
46. Zoeller RA, Morand OH, Raetz CR. A possible role for plasmalogens in protecting animal cells against photosensitized killing. J Biol Chem. 1988;263:11590–6.
47. Munn NJ, Arnio E, Liu D, Zoeller RA, Liscum L. Deficiency in ethanolamine plasmalogen leads to altered cholesterol transport. J lipid Res. 2003;44:182–92.
48. Honsho M, Abe Y, Fujiki Y. Dysregulation of plasmalogen homeostasis impairs cholesterol biosynthesis. J Biol Chem. 2015;290:28822–33.
49. Arenas F, Garcia-Ruiz C, Fernandez-Checa JC. Intracellular cholesterol trafficking and impact in neurodegeneration. Front Mol Neurosci. 2017;10:382.
50. Markesbery WR. The role of oxidative stress in alzheimer disease. Arch Neurol. 1999;56:1449–52.
51. Vance JE. Historical perspective: phosphatidylserine and phosphatidylethanolamine from the 1800s to the present. J Lipid Res. 2018;59:923–44.
52. Bazinet RP, Layé S. Polyunsaturated fatty acids and their metabolites in brain function and disease. Nat Rev Neurosci 2014;15:771–785.
53. Djuricic I, Calder PC. Beneficial outcomes of omega-6 and omega-3 polyunsaturated fatty acids on human health: an update for 2021. Nutrients. 2021;13:2421.
54. Díaz M, Mesa-Herrera F, Marín R. DHA and its elaborated modulation of antioxidant defenses of the brain: implications in aging and AD neurodegeneration. Antioxidants. 2021;10:907.
55. Tully AM, Roche HM, Doyle R, Fallon C, Bruce I, Lawlor B, et al. Low serum cholesteryl ester-docosahexaenoic acid levels in alzheimer's disease: a case–control study. Br J Nutr. 2003;89:483–9.
56. Sala-Vila A, Satizabal CL, Tintle N, Melo van Lent D, Vasan RS, Beiser AS, et al. Red blood Cell DHA is inversely associated with risk of incident alzheimer's disease and all-cause dementia: framingham offspring study. Nutrients. 2022;14:2408.
57. Nolan JM, Power R, Howard AN, Bergin P, Roche W, Prado-Cabrero A, et al. Supplementation with carotenoids, omega-3 fatty acids, and vitamin e has a positive effect on the symptoms and progression of alzheimer's disease. J Alzheimer's Dis. 2022;90:233–49.
58. Gustafson DR, Bäckman K, Scarmeas N, Stern Y, Manly JJ, Mayeux R, et al. Dietary fatty acids and risk of alzheimer's disease and related dementias: observations from the washington heights-hamilton heights-inwood columbia aging project (WHICAP). Alzheimer's Dement. 2020;16:1638–49.
59. Jun L, Najaf A, William S, Matthias A, Richa B, Bruno B et al. Longitudinal analysis of UK Biobank participants suggests age and APOE-dependent alterations of energy metabolism in development of dementia. medRxiv 2022.2002.2025.22271530.[Preprimt]. 2022. Available from: https://www.medrxiv.org/content/10.1101/2022.02.25.22271530v1
60. Giacobbe J, Benoiton B, Zunszain P, Pariante CM, Borsini A. The anti-inflammatory role of omega-3 polyunsaturated fatty acids metabolites in pre-clinical models of psychiatric, neurodegenerative, and neurological disorders. Front Psychiatry. 2020;11:122.
61. Zúñiga J, Venegas F, Villarreal M, Núñez D, Chandía M, Valenzuela R, et al. Protection against in vivo liver ischemia-reperfusion injury by n-3 long-chain polyunsaturated fatty acids in the rat. Free Radic Res. 2010;44:854–63.
62. Nagan N, Zoeller RA. Plasmalogens: biosynthesis and functions. Prog lipid Res. 2001;40:199–229.
63. Kou J, Kovacs GG, Höftberger R, Kulik W, Brodde A, Forss-Petter S, et al. Peroxisomal alterations in alzheimer's disease. Acta Neuropathol. 2011;122:271–83.
64. Jo DS, Park NY, Cho D-H. Peroxisome quality control and dysregulated lipid metabolism in neurodegenerative diseases. Exp Mol Med. 2020;52:1486–95.
65. Wójtowicz S, Strosznajder AK, Jeżyna M, Strosznajder JB. The novel role of PPAR alpha in the brain: promising target in therapy of alzheimer's disease and other neurodegenerative disorders. Neurochem Res. 2020;45:972–88.
66. Sagheddu C, Melis M, Muntoni AL, Pistis M. Repurposing peroxisome proliferator-activated receptor agonists in neurological and psychiatric disorders. Pharmaceuticals. 2021;14:1025.
67. Dodge JC, Tamsett TJ, Treleaven CM, Taksir TV, Piepenhagen P, Sardi SP, et al. Glucosylceramide synthase inhibition reduces ganglioside GM3 accumulation, alleviates amyloid neuropathology, and stabilizes remote contextual memory in a mouse model of alzheimer's disease. Alzheimers Res Ther. 2022;14:19–19.
68. Wang X, Bui H, Vemuri P, Graff-Radford J, Jack CR Jr, Petersen RC, et al. Lipidomic network of mild cognitive impairment from the mayo clinic study of aging. J Alzheimers Dis. 2021;81:533–43.
69. Chua XY, Torta F, Chong JR, Venketasubramanian N, Hilal S, Wenk MR, et al. Lipidomics profiling reveals distinct patterns of plasma sphingolipid alterations in alzheimer's disease and vascular dementia. Alzheimers Res Ther. 2023;15:214.
70. He Y, Huang SY, Wang HF, Zhang W, Deng YT, Zhang YR, et al. Circulating polyunsaturated fatty acids, fish oil supplementation, and risk of incident dementia: a prospective cohort study of 440,750 participants. Geroscience. 2023;45:1997–2009.

ACKNOWLEDGEMENTS

The data available in the AD Knowledge Portal would not be possible without the participation of research volunteers and the contribution of data by collaborating researchers. Metabolomics data as well as data preprocessing, analysis, and interpretation is provided by the Alzheimer's Disease Metabolomics Consortium (ADMC), part of the Accelerating Medicines Partnership for Alzheimer's Disease (AMP-AD), and funded wholly or in part by the following grants and supplements thereto: NIA Alzheimer's Disease Neuroimaging Initiative (ADNI) database (adni.loni.usc.edu),

RF1AG051550, RF1AG057452, R01AG059093, RF1AG058942, U01AG061359, U19AG063744 and FNIH: #DAOU16AMPA awarded to Dr. Kaddurah-Daouk at Duke University in partnership with a large number of academic institutions. A complete listing of ADMC investigators can be found at: https://sites.duke.edu/adnimetab/team/. Data on lipids was generated at Baker Heart and Diabetes Institute, a member of ADMC. Details on the lipid profiling technologies are described at: https://metabolomics.baker.edu.au/method/. Data collection and sharing for this project was funded by the Alzheimer's Disease Neuroimaging Initiative (ADNI) (National Institutes of Health Grant U01 AG024904) and DOD ADNI (Department of Defense award number W81XWH-12-2-0012). ADNI is funded by the National Institute on Aging, the National Institute of Biomedical Imaging and Bioengineering, and through generous contributions from the following: AbbVie, Alzheimer's Association; Alzheimer's Drug Discovery Foundation; Araclon Biotech; BioClinica, Inc.; Biogen; Bristol-Myers Squibb Company; CereSpir, Inc.; Cogstate; Eisai Inc.; Elan Pharmaceuticals, Inc.; Eli Lilly and Company; EuroImmun; F. Hoffmann-La Roche Ltd and its affiliated company Genentech, Inc.; Fujirebio; GE Healthcare; IXICO Ltd.; Janssen Alzheimer Immunotherapy Research & Development, LLC.; Johnson & Johnson Pharmaceutical Research & Development LLC.; Lumosity; Lundbeck; Merck & Co., Inc.; Meso Scale Diagnostics, LLC.; NeuroRx Research; Neurotrack Technologies; Novartis Pharmaceuticals Corporation; Pfizer Inc.; Piramal Imaging; Servier; Takeda Pharmaceutical Company; and Transition Therapeutics. The Canadian Institutes of Health Research is providing funds to support ADNI clinical sites in Canada. Private sector contributions are facilitated by the Foundation for the National Institutes of Health (www.fnih.org). The grantee organization is the Northern California Institute for Research and Education, and the study is coordinated by the Alzheimer's Therapeutic Research Institute at the University of Southern California. ADNI data are disseminated by the Laboratory for Neuro Imaging at the University of Southern California. This research was supported by a grant from the Korea National Institute of Health (KNIH), Korea Disease Control and Prevention Agency (KDCA) (grant number 2023-ER1001-03). Additional funding for analysis was provided by several awards from the NIA (U19 AG024904, P30 AG072976, U19 AG074879, U01AG068057 and U01AG072177).

AUTHOR CONTRIBUTIONS

JPK and KN designed the study, performed the statistical analyses, and wrote the manuscript. TW contributed to data processing and interpretation. SLR contributed to neuroimaging data acquisition and processing. XH and BSK contributed to lipidomics methodology and data interpretation. MA, GK, CB, and RB contributed to data management and quality control. PJM and KH supervised lipid data generation and contributed to interpretation. PJB critically reviewed the manuscript for language, clarity, and scientific expression. AJS and RKD conceptualized and supervised the study, acquired funding, and critically revised the manuscript. All authors reviewed and approved the final version of the manuscript.

COMPETING INTERESTS

Dr. Kaddurah-Daouk is an inventor on a series of patents on use of metabolomics for the diagnosis and treatment of CNS diseases and holds equity in Metabolon Inc., Chymia LLC and PsyProtix.

ADDITIONAL INFORMATION

Supplementary information The online version contains supplementary material available at https://doi.org/10.1038/s41380-026-03626-z.

Correspondence and requests for materials should be addressed to Andrew J. Saykin or Rima Kaddurah-Daouk.

Reprints and permission information is available at http://www.nature.com/reprints

Publisher's note Springer Nature remains neutral with regard to jurisdictional claims in published maps and institutional affiliations.

FOR THE ALZHEIMER'S DISEASE NEUROIMAGING INITIATIVE

Michael Weiner[15], Paul Aisen[16], Ronald Petersen[17], Clifford R. Jack Jr[17], William Jagust[18], Susan Landau[18], Monica Rivera-Mindt[19], Ozioma Okonkwo[20], Leslie M. Shaw[21], Edward B. Lee[21], Arthur W. Toga[16], Laurel Beckett[22], Danielle Harvey[22], Robert C. Green[23], Andrew J. Saykin[24], Kwangsik Nho[24], Richard J. Perrin[25], Duygu Tosun[15], Nick C. Fox[26], Paul Thompson[27], Charles DeCarli[22], Robert A. Koeppe[28], Gil Rabinovici[15], John Morris[25], Nigel J. Cairns[25], Tatiana M. Foroud[24], Shannon L. Risacher[24], Rima Kaddurah-Daouk[29], Neil Buckholtz[30], John K. Hsiao[30], Laurie Ryan[30] and Susan Molchan[30]

[15]University of California, San Francisco, San Francisco, CA, USA. [16]University of Southern California, Los Angeles, CA, USA. [17]Mayo Clinic, Rochester, MN, USA. [18]University of California, Berkeley, Berkeley, CA, USA. [19]Fordham University, New York, NY, USA. [20]University of Wisconsin, Madison, WI, USA. [21]University of Pennsylvania, Philadelphia, PA, USA. [22]University of California, Davis, Davis, CA, USA. [23]Boston University, Boston, MA, USA. [24]Indiana University School of Medicine, Indianapolis, IN, USA. [25]Washington University in St. Louis, St. Louis, MO, USA. [26]University College London, London, UK. [27]UCLA School of Medicine, Los Angeles, CA, USA. [28]University of Michigan, Ann Arbor, MI, USA. [29]Duke University, Durham, NC, USA. [30]National Institute on Aging, Bethesda, MD, USA

ALZHEIMER'S DISEASE METABOLOMICS CONSORTIUM (ADMC)

Rima Kaddurah-Daouk[29], Alexandra Kueider-Paisley[29], P. Murali Doraiswamy[29], Colette Blach[29], Arthur Moseley[29], Siamak Mahmoudiandehkhordi[29], Kathleen Welsh-Balmer[29], Brenda Plassman[29], Andrew J. Saykin[24], Kwangsik Nho[24], Shannon Risacher[24], Gabi Kastenmüller[31], Matthias Arnold[31], Xianlin Han[8], Rebecca Baillie[32], Rob Knight[33], Pieter Dorrestein[33], James Brewer[33], Emeran Mayer[34], Jennifer Labus[34], Pierre Baldi[34], Arpana Gupta[34], Oliver Fiehn[35], Dinesh Barupal[36], Peter Meikle[3], Sarkis Mazmanian[37], Dan Rader[21], Leslie Shaw[21], Cornelia van Duijn[38], Najaf Amin[38], Alejo Nevado-Holgado[38], David Bennett[39], Ranga Krishnan[39], Ali Keshavarzian[39], Robin Vogt[39], Arfan Ikram[40], Thomas Hankemeier[41], Ines Thiele[42], Cory Funk[43], Priyanka Baloni[44], Wei Jia[45], David Wishart[46], Roberta Brinton[47], Lindsay Farrer[23], Rhoda Au[23], Wendy Qiu[23], Peter Würtz[48], Therese Koal[49], Anna Greenwood[50], Jan Krumsiek[51], Karsten Suhre[52], John Newman[53], Ivan Hernandez[54], Tatiana Foroud[55] and Frank Sacks[56]

[31]Helmholtz Zentrum München, Neuherberg, Germany. [32]Rosa & Co., LLC, San Carlos, CA, USA. [33]University of California, San Diego, San Diego, CA, USA. [34]University of California, Los Angeles, Los Angeles, CA, USA. [35]West Coast Metabolomics Center, University of California, Davis, Davis, CA, USA. [36]Icahn School of Medicine at Mount Sinai, New York, NY, USA. [37]California Institute of Technology, Pasadena, CA, USA. [38]University of Oxford, Oxford, UK. [39]Rush University, Chicago, IL, USA. [40]Erasmus MC, Rotterdam, The Netherlands. [41]Leiden University Metabolomics Center, Leiden, The Netherlands. [42]National University of Ireland – Galway, Galway, Ireland. [43]Institute for Systems Biology, Seattle, WA, USA. [44]Purdue University, West Lafayette, IN, USA. [45]University of Hawaii Cancer Center, Honolulu, HI, USA. [46]The Metabolomics Innovation Centre (TMIC), Edmonton, Alberta, Canada. [47]University of Arizona, Tucson, AZ, USA. [48]Nightingale Health, Helsinki, Finland. [49]Biocrates Life Sciences AG, Innsbruck, Austria. [50]Sage Bionetworks, Seattle, WA, USA. [51]Weill Medical College of Cornell, New York, NY, USA. [52]Weill Cornell Medicine-Qatar, Doha, Qatar. [53]USDA ARS, Washington, DC, USA. [54]SUNY Downstate, Brooklyn, NY, USA. [55]National Centralized Repository for Alzheimer's and other Dementias (NCRAD), Indianapolis, IN, USA. [56]Harvard School of Public Health (Harvard T.H. Chan School of Public Health), Boston, MA, USA.